

Submitted to Astron.J.

A Color-Magnitude Diagram for a Globular Cluster in the Giant Elliptical Galaxy NGC 5128

Gretchen L. H. Harris and G. B. Poole

Department of Physics, University of Waterloo
Waterloo ON N2L 3G1, Canada; glharris,gbpoole@astro.uwaterloo.ca

and

William E. Harris

Department of Physics and Astronomy, McMaster University
Hamilton ON L8S 4M1, Canada; harris@physics.mcmaster.ca

ABSTRACT

The *Hubble Space Telescope* has been used to obtain WFPC2 (V, I) photometry for a large sample of stars in the outer halo of the giant elliptical NGC 5128, at a distance 4 Mpc beyond the Local Group. The globular cluster N5128-C44, at the center of the Planetary Camera field, is well enough resolved to permit the construction of a color-magnitude diagram (CMD) for it which covers the brightest two magnitudes of the giant branch. The CMD is consistent with that of a normal old, moderately low-metallicity ($[\text{Fe}/\text{H}] \simeq -1.3$) globular cluster, distinctly more metal-poor than most of the field halo stars at the same projected location (which average $[\text{Fe}/\text{H}] \sim -0.5$). This is the most distant globular cluster in which direct color-magnitude photometry has been achieved to date, and the first one belonging to a giant E galaxy.

Subject headings: galaxies: elliptical and lenticular — galaxies: star clusters

1. Introduction

Globular clusters are typically found in much larger numbers within giant elliptical galaxies than in large spirals such as the Milky Way or M31, and in extreme cases such as cD galaxies the total population can exceed 20,000 clusters per galaxy (*e.g.* W. Harris 1991). It is conventionally assumed that the clusters in these remote galaxies must individually resemble the familiar Milky Way old-halo globulars in their ages, metallicities, and stellar compositions. But making direct tests of this fundamental assumption in different galaxies is a difficult task. For even the closest large galaxy, M31, it has become possible only recently to study the stellar compositions of its

old-halo clusters through direct color-magnitude photometry (*e.g.*, Fusi Pecci *et al.* 1996; Rich *et al.* 1996). The situation is worse for giant E galaxies, which are all far beyond the Local Group and in which individual clusters are seen as no more than faint, unresolved semi-stellar objects even under the best imaging conditions. The only reasonably direct tests of their nature are ones based on integrated light – color indices, spectral properties, line strengths – which verify that their characteristics at least roughly match those of the Milky Way globulars (see, *e.g.*, Cohen *et al.* 1997 for a comprehensive recent spectroscopic study of clusters in M87; or Jablonka *et al.* 1996 for spectral characteristics of clusters in NGC 5128). However, the information derived from integrated light must, by definition, be heavily smoothed over the composite stellar population. A color-magnitude diagram (CMD) for any such object, even with limited depth, would provide a uniquely direct test of their nature.

2. Observations

By far the closest giant elliptical galaxy is NGC 5128, the dominant member of the Centaurus group at $d \sim 4$ Mpc (the next nearest gE is NGC 3379 in the Leo group, which at $d \sim 10$ Mpc is a full two magnitudes more distant). Although its innermost few kiloparsecs are affected by the well known dust lanes and gas, the main body of the galaxy and its extensive halo are by all indications those of a basically normal giant elliptical (*e.g.*, Graham 1979; Ebneter & Balick 1983; Hui *et al.* 1995; Soria *et al.* 1996; Storchi-Bergmann *et al.* 1997). Since interactions and mergers of the type now happening in NGC 5128 are now recognized to be rather common occurrences in the ongoing histories of large galaxies, it is entirely reasonable to expect that its underlying stellar composition will be typical of gE’s. In addition, its population of ~ 1500 globular clusters (G. Harris *et al.* 1984) has color and luminosity distributions that clearly resemble the clusters found in other, more remote gE’s such as in Virgo and Fornax (see G. Harris *et al.* 1992 [hereafter HGHH], Hesser *et al.* 1984, and H. Harris *et al.* 1988). NGC 5128 unquestionably offers our best chance to investigate globular clusters in a giant E galaxy in the best possible depth and detail.

In HST/WFPC2 program GO-5905, executed in two visits on 1997 Aug 16 and 24, we obtained deep images of a field in the outer halo of NGC 5128. The PC1 CCD was centered on the globular cluster N5128-C44, which is located at a projected distance of $R_{gc} = 18'32$ from the center of NGC 5128, equivalent to $21.3(d/4)$ kpc. This location in the halo is far outside the core regions contaminated by the dust lanes and thus should be representative of the old-halo population of the elliptical (see HGHH for complete wide-field finder charts and a compilation of the relevant cluster data). C44 itself is a luminous, moderately low-metallicity cluster according to the photometry published in HGHH: at an integrated magnitude $V = 18.48$ ($M_V = -9.87$ for a distance modulus $(m - M)_V = 28.35$; see below) it is similar to the luminous halo globulars in the Milky Way such as M3 or NGC 2419, while its $(C - T_1)$ color yields an estimated metallicity $[\text{Fe}/\text{H}] = -1.4 \pm 0.25$, quite similar to the mean metallicity of the Milky Way halo clusters and field stars. Lastly, the cluster radial velocity of 520 km s^{-1} is almost identical with the systemic

mean of $\sim 540 \text{ km s}^{-1}$ for its host galaxy (HGHH; H. Harris *et al.* 1988; Hesser *et al.* 1986).

Our WFPC2 observations consisted of 10 images totalling 12800 seconds in each of the two standard filters F606W (V) and F814W (I), with individual exposures sub-pixel shifted over five separate positions. The images were reregistered and combined to form composite deep (V, I) images free of cosmic rays and bad pixels. By simultaneously imaging both a metal-poor globular cluster and the halo field stars, our original intention was to gain the most direct possible comparison between their two mean metallicities, as well as to give us an additional consistency check on the metallicity scale from our ($V - I$) colors. Our photometry from the WF2,3,4 images has been used to generate a color-magnitude diagram (CMD) for the galaxy halo, covering about 2.5 magnitudes of the old red giant branch (RGB) and containing more than 10,000 stars. That material is described in a companion paper along with a more detailed outline of the data reduction (G. Harris *et al.* 1998); here, we present the results for the PC1 field and the globular cluster.

In the following discussion, we adopt a distance to NGC 5128 of 4.0 Mpc, based on planetary nebula luminosity functions (Hui *et al.* 1993), surface brightness fluctuations (Tonry & Schechter 1990; Hui *et al.* 1993), and the luminosity of the RGB tip (G. Harris *et al.* 1998; Soria *et al.* 1996), all normalized to a contemporary Local Group distance scale in which $d(M31) = 770 \text{ kpc}$ (*e.g.*, van den Bergh 1995; Fernley *et al.* 1998; and references cited there). The foreground reddening is adopted as $E(B - V) = 0.11$ and $E(V - I) = 0.14$, giving $(m - M)_V = 28.35$.

3. Data Reduction

The image of the PC field around C44 is shown in Figure 1. The cluster subtends only a small angle (at $d = 4 \text{ Mpc}$, typical globular cluster core and tidal radii of $r_c \sim 2 \text{ pc}$, $r_t \sim 50 \text{ pc}$ would have angular sizes of $0''.1$ and $2''.5$, superimposed on the PC1 image scale of $0''.046$ per pixel). Thus almost all of its stars are severely crowded and stellar photometry is restricted to the brighter stars on its outskirts. But the task is not hopeless. An excellent analogy of what we can expect to accomplish is to compare with the globular clusters in M31: in terms of spatial resolution and scale, imaging M31 *from the ground* under good seeing conditions of $\simeq 0''.5$ is closely comparable with imaging NGC 5128 (5 times more distant) with the $0''.1$ -resolution of HST. Successful ground-based studies of several M31 clusters were indeed achieved in the pre-HST era (Couture *et al.* 1995; Heasley *et al.* 1988; Christian & Heasley 1991). In any one of these clusters, typically two or three dozen of the RGB stars could be isolated and measured, with representative photometric scatter of $\sigma(V - I) = \pm 0.2 - 0.3$ driven by the crowding and background nonuniformity. Although the precision of these studies was unavoidably low, it is important to note that the subsequent much deeper and more precise photometry carried out later with HST (see, *e.g.*, Fusi Pecci *et al.* 1996; Rich *et al.* 1996) verified that this pioneering ground-based photometry was able to produce *systematically* accurate colors and mean RGB loci.

We first extracted a 190×190 pixel subsection ($8''.74 \times 8''.74$) from the PC1 image, centered on C44 (Figure 1). To eliminate as much of the unresolved light of the cluster as possible, we used the ellipse-fitting code within STSDAS to derive an isophotal contour model for the cluster, and subtracted this from the raw image. The result (second panel of Figure 1) was then used for stellar photometry through the DAOPHOT II code (Stetson 1992). Three iterations of the usual sequence FIND/PHOT/ALLSTAR were employed, along with a very small psf-fitting radius (0.8 fwhm), to find and extract the individual stars near the cluster. As a check on this procedure, we also tried removing the unresolved cluster light by a first pass of finding and removing stars, smoothing the remaining light by median filtering, subtracting that from the original image, and repeating the process (see Couture et al. 1995). The overall results for the stellar photometry were quite similar; however, the first (ellipse-fitting) procedure allowed us to reach slightly further in toward cluster center and to define the CMD a little more narrowly.

Zeropoints and color terms for the conversion of instrumental magnitudes into (V, I) followed the prescriptions of Holtzman *et al.* (1995) and are discussed completely in G. Harris *et al.* (1998).

4. The Color-Magnitude Diagram

The resulting CMD is shown in Figure 2, in which all measured data points are plotted without any selection criteria applied. The stars closest to the cluster ($r < 1''.4 \simeq 30$ px, which we will call the “inner zone”) are systematically bluer than the surrounding field-halo stars, suggesting that this particular cluster has distinctly lower metallicity than the average of the halo stars. To define a cleaner CMD for the cluster, we culled the data in two additional ways: (a) stars with very poor goodness-of-fit values ($\chi > 4$, although the great majority of stars had $\chi < 2$) were eliminated; and (b) individual stars were removed from the inner-zone CMD in proportion to their presence in the outer ($r > 30$ px) zone. For this latter step, we divided the CMD into a grid of boxes of size $\Delta I \simeq 0.5$, $\Delta(V - I) \simeq 0.2$. Then, noting that the area of the outer zone (70.0 arcsec^2) is ~ 11 times larger than that of the inner zone (6.4 arcsec^2), we removed one star from the inner-zone CMD in any box which also contained $\sim 10 \pm 3$ stars from the outer zone. (This star-by-star extraction will actually remove too *few* stars for $I \gtrsim 25.5$, where the detection completeness is much lower in the highly crowded cluster than in the surrounding field. Thus we expect the fainter parts of the cluster CMD to remain partially contaminated, but by only two or three stars at worst.)

The “cleaned” CMD for the cluster is shown in Figure 3. The 45 remaining points now scatter more closely around the fiducial line for $[\text{Fe}/\text{H}] = -1.3$ over the 2.5-magnitude run of the data, particularly at the bright RGB tip where the stellar photometry should be the most reliable. This metallicity estimate is uncertain by perhaps $\simeq \pm 0.3$ dex taking into consideration both the random photometric scatter and the uncertainties in reddening and distance moduli; but it is entirely consistent with the previous metallicity calibration $[\text{Fe}/\text{H}]_{C-T_1} = -1.4$ from its integrated colors (HGHH). The typical color uncertainty $\sigma(V - I) \simeq \pm 0.15 - 0.2$ per star, along with some

residual contamination by field stars, is enough to be responsible for the remaining scatter we see in the CMD.

5. Radial Profile and Structural Parameters

Cluster C44 is sufficiently extended on the PC1 image that we can make useful estimates of its structural parameters. The smooth profile of the cluster light generated from our *stsdas.ellipse* and *.bmodel* fits is shown in Figure 4. Both the V and I surface intensity plots indicate that the core of the cluster is significantly more extended than the PSF profile, and at large radii, the light can be traced out past $r \sim 2''$ (40 px). The profile shape is also nearly circular and fairly uniform with radius, as shown in Figure 5; the eccentricity of the model fit goes through modest fluctuations about its mean value $\langle e \rangle \simeq 0.06$.

Comparison with representative King (1966) model profile curves, also shown in Figure 4, indicates that the cluster is adequately matched by models with central potential parameters in the range $W_0 = 7 \pm 1$. A *very rough* estimate of the core radius of the cluster from the model fits is $r_c \simeq 0''.08 \simeq 1.5$ pc, after subtraction in quadrature of the PSF “core” $r_{c,PSF} \simeq 0''.04$. The half-mass radius, which is larger and thus more well determined, is at $r_h \simeq 0''.27 \simeq 5$ pc, and the central concentration index of the fitted curve is $c = \log(r_t/r_c) = 1.6 \pm 0.3$. Its estimated tidal radius is then $r_t \sim 3'' \sim 60$ pc. These values all lie comfortably within the typical range for globular clusters in the outer halo of the Milky Way, which have more extended cores and larger tidal radii than those in the inner bulge (*e.g.*, Trager *et al.* 1995; van den Bergh *et al.* 1991).

In summary, this study clearly favors the important “null hypothesis” that N5128-C44 is an old, metal-poor globular cluster closely resembling the familiar ones in the Milky Way in every way we can test it: metallicity, integrated color, color-magnitude diagram, and King-like structural parameters. This is the first time that direct stellar photometry has been used to test this hypothesis in any globular cluster in a giant E galaxy. Our results support the contention that we are genuinely dealing with the same fundamental type of object when we perform comparisons between old-halo globular cluster populations in gE galaxies and those in the Local Group. We suggest that the photometric analysis of globular clusters in other galaxies well beyond the Local Group is within reach, and will become routine with the deployment of more advanced imaging tools.

We are grateful for technical advice from Pat Durrell and Dean McLaughlin. This work was supported financially by the Natural Sciences and Engineering Research Council of Canada, through operating grants to G.L.H.H. and W.E.H.

REFERENCES

- Christian, C. A., & Heasley, J. N. 1991, *AJ*, 101, 848
- Cohen, J. G., Blakeslee, J. P., & Ryzhov, A. 1997, *ApJ*, 496, 808
- Couture, J., Racine, R., Harris, W. E., & Holland, S. 1995, *AJ*, 109, 2050
- Da Costa, G., & Armandroff, T. 1990, *AJ*, 100, 162
- Ebner, K., & Balick, B. 1983, *PASP*, 95, 675
- Fernley, J. *et al.* 1998, *A&A*, 330, 515
- Fusi Pecci, F., *et al.* 1996, *AJ*, 112, 1461
- Graham, J. A. 1979, *ApJ*, 232, 60
- Guarnieri, A., Clementini, G., Valentini, G., Castro-Tirado, A., Gorosabel, J., & Pedrosa, A. 1998, *A&A*, 331, 70
- Harris, G. L. H., Hesser, J. E., Harris, H. C., & Curry, P. J. 1984, *ApJ*, 287, 175
- Harris, G. L. H., Geisler, D., Harris, H. C., & Hesser, J. E. 1992, *AJ*, 104, 613 (HGHH)
- Harris, G. L. H., Harris, W. E., & Poole, G. B. 1998, in preparation
- Harris, H. C., Harris, G. L. H., & Hesser, J. E. 1988, in *Globular Cluster Systems in Galaxies*, IAU Symposium No. 126, ed. J. E. Grindlay & A. G. D. Philip (Dordrecht: Kluwer), 205
- Harris, W. E., *ARA&A*, 29, 543
- Heasley, J. N., Christian, C. A., Friel, E. D., & Janes, K. A. 1988, *AJ*, 96, 1312
- Hesser, J. E., Harris, H. C., & Harris, G. L. H. 1986, *ApJ*, 303, L51
- Hesser, J. E., Harris, H. C., van den Bergh, S., & Harris, G. L. H. 1984, *ApJ*, 276, 491
- Holtzman, J. A. 1995, *PASP*, 107, 1065
- Hui, X., Ford, H. C., Ciardullo, R., & Jacoby, G. H. 1993, *ApJ*, 414, 463
- Hui, X., Ford, H. C., Freeman, K. C., & Dopita, M. A. 1995, *ApJ*, 449, 592
- Jablonka, P., Bica, E., Pelat, D., & Alloin, D. 1996, *A&A*, 307, 385
- King, I. R. 1966, *AJ*, 71, 64
- Rich, R. M., Mighell, K. J., Freedman, W. L., & Neill, J. D. 1996, *AJ*, 111, 768

Soria, R. *et al.* 1996, ApJ, 465, 79

Stetson, P.B. 1992, in *Astronomical Data Analysis Software and Systems I*, ASP Conf.Ser. Vol.8, edited by G.H.Jacoby (ASP, San Francisco), p. 289

Storchi-Bergmann, T., Bica, E., & Kinney, A. L. 1997, MNRAS, 290, 231

Tonry, J. L., & Schechter, P. L. 1990, AJ, 100, 1794

Trager, S. C., King, I. R., & Djorgovski, S. 1995, AJ, 109, 218

van den Bergh, S. 1995, ApJ, 446, 39

van den Bergh, S., Morbey, C., & Pazder, J. 1991, ApJ, 375, 594

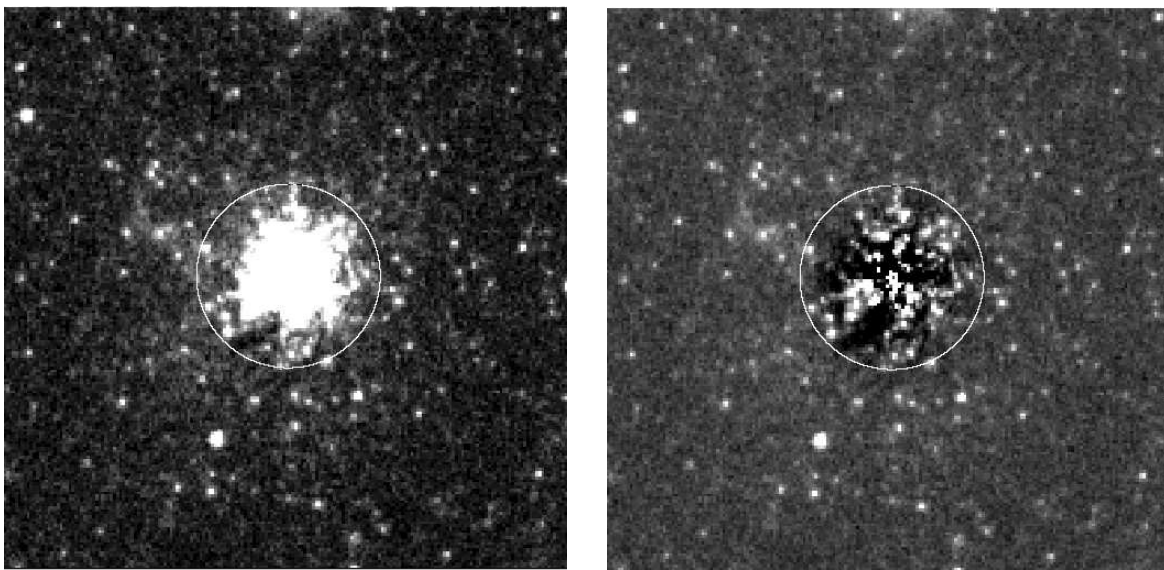


Fig. 1.— (a) *First panel:* The central 190×190 pixels ($8''.7 \times 8''.7$) of the Planetary Camera WFPC2 field, centered on globular cluster C44 in the halo of NGC 5128. The image is a 12800-second sum of 10 exposures in V (F606W). The smooth unresolved light of the cluster has been partially subtracted to emphasize the resolution into stars of its outer envelope. The inscribed circle denotes the radius ($30 \text{ px} = 1''.4$) of the inner zone used to define the cluster CMD. (b) *Second panel:* The same PC1 field after removal of elliptical isophotes.

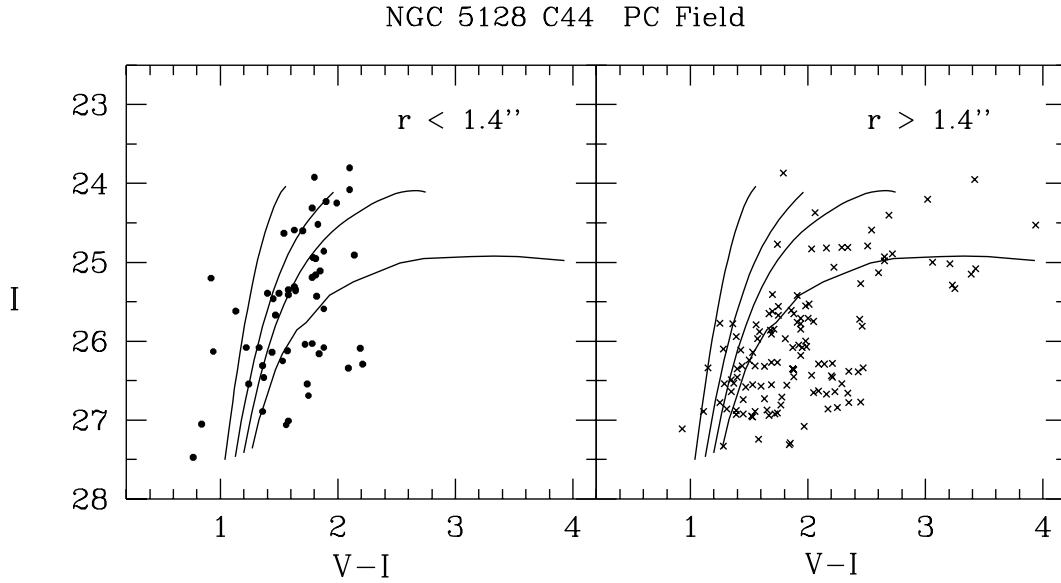


Fig. 2.— Color-magnitude data for all measured stars in the central PC field. Solid dots (left panel) denote stars within the inner 30-px ($1''.4$) circle; crosses (right panel) denote objects outside that circle, which are mostly RGB stars in the halo of NGC 5128. The four lines superimposed on the diagram are fiducial lines for Milky Way globular clusters of four different metallicities (Da Costa & Armandroff 1990; Guarnieri et al. 1998); from left to right, they are M15 ($[\text{Fe}/\text{H}] = -2.2$), NGC 1851 (-1.3), 47 Tuc (-0.7), and NGC 6553 (-0.25). The lines have been placed assuming an intrinsic distance modulus for NGC 5128 of $(m - M)_0 = 28.0$ and reddening $E(V - I) = 0.14$ (see text).

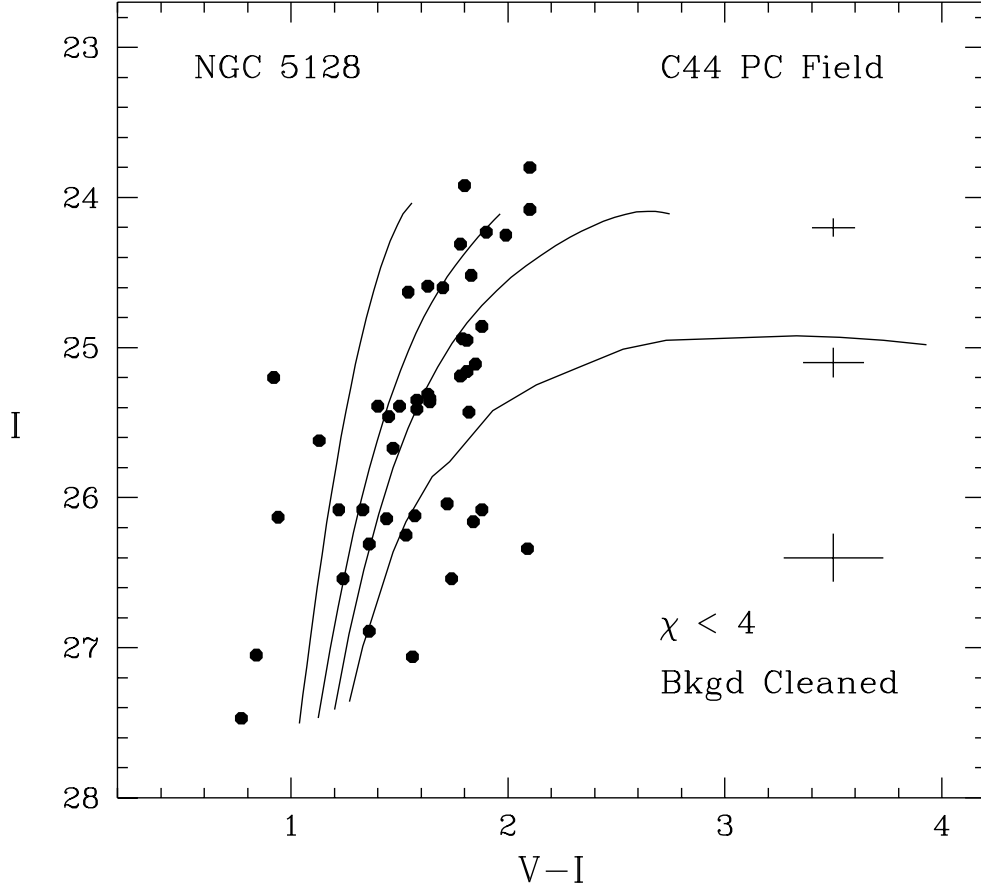


Fig. 3.— Statistically cleaned CMD for the globular cluster C44. Stars with poor PSF fits ($\chi > 4$) have been rejected, and background contamination in proportion to the area of the inner zone has been removed as described in the text. The fiducial cluster sequences for four different metallicities are the same as in Fig. 2. Photometric measurement uncertainties from the ALLSTAR fitting algorithms are indicated for three different magnitude levels by the error bars at right. C44 appears to have a moderately low metallicity $[\text{Fe}/\text{H}] \simeq -1.3$ based on the color of its RGB, and in close agreement with the metallicity from its integrated $(C - T_1)$ color index.

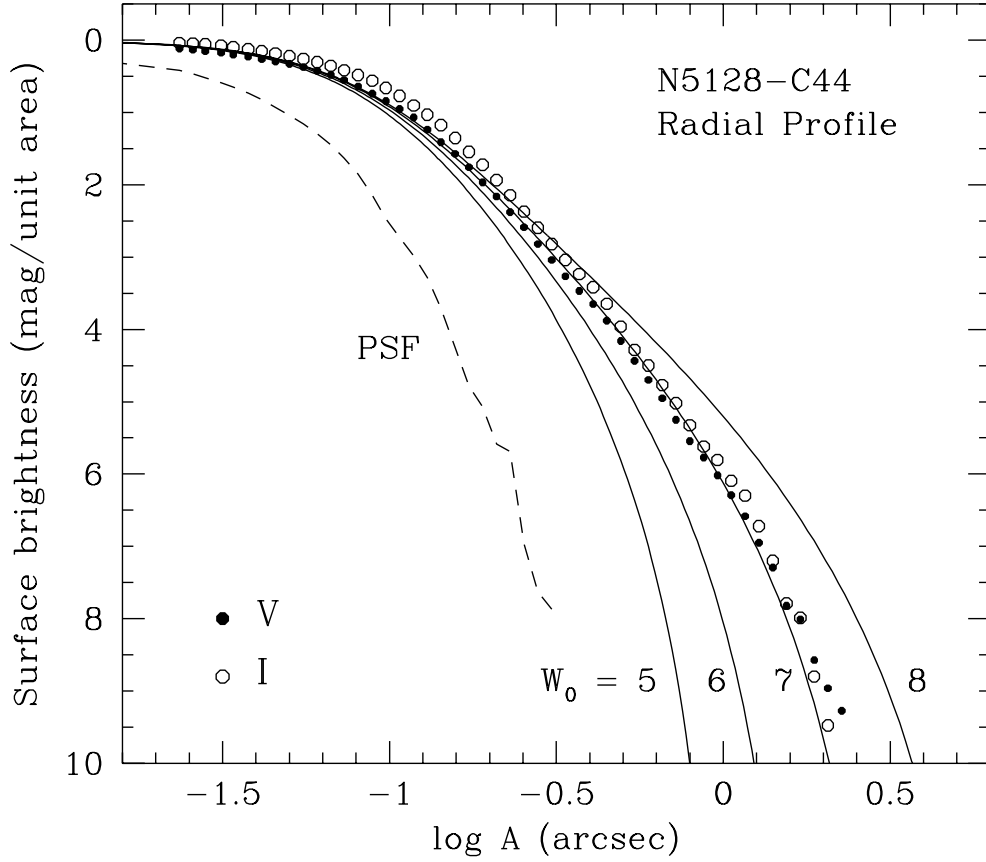


Fig. 4.— Radial profile of the cluster light, plotted as surface brightness (magnitudes per unit area relative to the central intensity) against $\log A$ (semi-major axis) in arcseconds. *Solid dots* denote the surface intensity in V of the smoothed isophotal model of the cluster; *open circles* denote the intensity profile in I . The dashed line at left shows the profile of the stellar point-spread function. *Solid lines* superimposed on the data points are profiles for four King models with different values of the central potential parameter W_0 (curves of increasing central concentration go from left to right). We estimate the cluster to have a core radius $r_c \simeq 0''.08$ (about twice as large as the PSF core) and tidal radius $r_t \simeq 3''$.

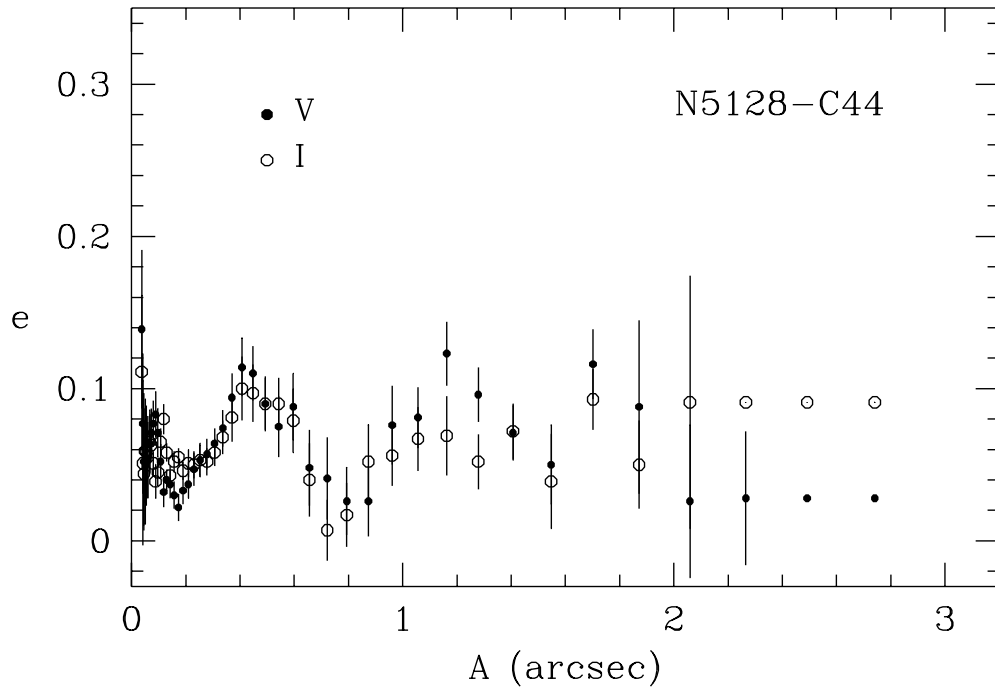


Fig. 5.— Eccentricity e of the cluster profile, as a function of semi-major axis A . The e -values are deduced from the elliptical isophote fit to the cluster light described in the text. The cluster has a small and nearly uniform eccentricity $\langle e \rangle \simeq 0.06$.